Optically stimulated luminescence (OSL) dosimetry in medicine

2008 Phys. Med. Biol. 53 R351

(http://iopscience.iop.org/0031-9155/53/20/R01)

IOP PUBLISHING PHYSICS IN MEDICINE AND BIOLOGY

Phys. Med. Biol. **53** (2008) R351–R379 doi:10.1088/0031-9155/53/20/R01

TOPICAL REVIEW

Optically stimulated luminescence (OSL) dosimetry in medicine

E G Yukihara and S W S McKeever

Department of Physics, Oklahoma State University, Stillwater, OK 74078, USA

E-mail: eduardo.yukihara@okstate.edu

Received , in final form 19 August 2008
Published 17 September 2008
Online at stacks.iop.org/PMB/53/R351

Abstract

This paper reviews fundamental and practical aspects of optically stimulated luminescence (OSL) dosimetry pertaining to applications in medicine, having particularly in mind new researchers and medical physicists interested in gaining familiarity with the field. A basic phenomenological model for OSL is presented and the key processes affecting the outcome of an OSL measurement are discussed. Practical aspects discussed include stimulation modalities (continuous-wave OSL, pulsed OSL and linear modulation OSL), basic experimental setup, available OSL readers, optical fiber systems and basic properties of available OSL dosimeters. Finally, results from the recent literature on applications of OSL in radiotherapy, radiodiagnostics and heavy charged particle dosimetry are discussed in light of the theoretical and practical framework presented in this review. Open questions and future challenges in OSL dosimetry are highlighted as a guide to the research needed to further advance the field.

(Some figures in this article are in colour only in the electronic version)

1. Introduction

Optically stimulated luminescence dosimeters (OSLDs) are now well established in personal dosimetry, having been already used commercially for almost a decade. The operation principle is identical to the well-known thermoluminescence dosimeters (TLDs), except that the readout is performed by controlled illumination of the dosimeter instead of by heating. The appeal of the OSL technique, at least in personal dosimetry, stems from the high sensitivity of carbon-doped aluminum oxide (Al_2O_3:C), the rapid and well-controlled optical readout and the possibility of re-estimating the absorbed dose.

The optically stimulated luminescence (OSL) technique itself has been used for the estimation of the environmental dose using naturally occurring minerals in luminescence dating since first proposed by Huntley *et al* (1985). The application of OSL in luminescence

dating and retrospective dosimetry led to the development of readers capable of automatically carrying out OSL measurements on large numbers of samples (Bøtter-Jensen 1997) and helped promote the technique. The introduction of carbon-doped aluminum oxide (Al_2O_3:C), initially suggested as a highly sensitive TL material (Akselrod *et al* 1990), finally provided an OSL material with attractive characteristics for personal dosimetry. More sophisticated readout approaches that employ fast time discrimination to separate the OSL from the stimulation light—namely, the pulsed OSL (POSL) technique—were proposed to take advantage of the properties of Al_2O_3:C (Akselrod and McKeever 1999). In 1998, the first commercial OSL dosimetry service based on Al_2O_3:C and the POSL technique (Luxel^{TM}) was introduced by Landauer Inc[1]. More recently, commercial readers specifically designed for dosimetry have become available (Bøtter-Jensen *et al* 2003, Perks *et al* 2007).

The application of OSL in medicine is still incipient, but slowly increasing. For instance, the number of presentations on OSL at the American Association of Physicists in Medicine (AAPM) annual meetings was two in 2005, three in 2006 and seven in 2007. Although these numbers are a narrow indicator of the research activity on medical applications of OSL, there is a noticeable increase in the number of papers and groups involved in OSL research. A few more in-depth investigations on the performance of OSLDs used as passive dosimeters in radiotherapy are now available (Jursinic 2007, Schembri and Heijmen 2007, Yukihara *et al* 2007, Viamonte *et al* 2008). Moreover, the International Atomic Energy Agency (IAEA) currently coordinates a research project to develop procedures for *in vivo* dosimetry in radiotherapy which includes a comparison between the OSL and other established techniques and involves groups from different countries (IAEA CRP Number: E2.40.14)[2]. The complete results from the IAEA study should be available soon.

In addition to OSLDs used as passive dosimeters, the optical readout allows the interrogation of the OSLDs using optical fibers. Prototype systems using optical fibers have been developed for real-time *in vivo* dosimetry and quality assurance in radiotherapy and radiodiagnostics (Huston *et al* 2001, Ranchoux *et al* 2002, Andersen *et al* 2003, Aznar *et al* 2004, Polf *et al* 2002, 2004, Gaza *et al* 2004, 2005). These real-time applications open a range of possibilities, taking advantage not only of common OSLD materials such as Al_2O_3:C, but also other materials characterized by significant fading at room temperature (Gaza and McKeever 2006, Klein and McKeever 2007).

OSLDs have also been investigated for heavy charged particle (HCP) dosimetry in space and charged particle therapy, both challenging problems. In proton therapy, for example, the use of range shifters to create the so-called spread-out Bragg peak (SOBP) in practice means that the dose at any point is deposited by particles with different energies and consequently different linear energy transfers (LETs). The problem is that the relative response (luminescence efficiency) of TLDs and OSLDs varies with LET and with the particular energy distribution inside the detectors, therefore requiring corrections. The possibility of using OSLDs for precise dosimetry in proton and carbon therapy has yet to be demonstrated, although the first steps in this direction have been taken using optical fiber systems (Edmund *et al* 2007, Andersen *et al* 2007).

This paper reviews fundamental and practical aspects of OSL dosimetry relevant to applications in medicine, having particularly in mind new researchers and medical physicists interested in gaining familiarity with the field. We also discuss the available results from radiotherapy, radiodiagnostics and HCP dosimetry, highlighting how they are related to the practical aspects presented in earlier sections. Although most of the literature is focused on

[1] http://www.osldosimetry.com/introduction (accessed on 14 December 2007).
[2] http://www-naweb.iaea.org/nahu/dmrp/crp.asp (accessed on 17 November 2007).

medical applications, the discussion is also relevant for dosimetry of biological experiments. For more in-depth or complementary information on OSL dosimetry, we refer to McKeever (2001), Bøtter-Jensen *et al* (2003), McKeever and Moscovitch (2003) and Akselrod *et al* (2007). Image plates and photostimulable phosphors have been reviewed elsewhere and will not be discussed here (Rowlands 2002).

2. Theoretical and practical aspects

2.1. Basic phenomenological model

To understand how the OSL signal is produced and to appreciate those physical and experimental aspects affecting the outcome of an OSL measurement, it is important to have at least a simple, phenomenological model that describes and incorporates the main processes taking place in the dosimeter during irradiation and readout.

The OSL phenomenon can be explained within the same framework used to explain the TL process, but adding additional optical transitions that can occur when the material is exposed to light. The energy levels in the crystalline structure of the dosimeter consist of delocalized energy bands, the most important in our case being the valence and conduction bands, created by the periodic potential of the crystal. The conduction and valence bands are separated by a band gap, the so-called forbidden band, in which only localized energy levels introduced by defects in the crystalline structure can exist (Bube 1960). Ionizing radiation is capable of exciting electrons to the conduction band, leaving behind holes in the valence band. The electrons in the conduction band and the holes in the valence band are free to move in the crystal lattice until they recombine with each other or are captured by the localized energy levels, which act as traps. The trapped charge concentration at these localized energy levels provides a record of the total dose absorbed by the crystal. This record can be 'read' by stimulating the trapped charges back to the conduction band, which results in electron–hole pair recombination and luminescence. Thus, the stimulated luminescence intensity is a surrogate for the trapped charge concentration and, thereby, the absorbed dose.

The processes described above are illustrated in figure 1, which, in addition to the conduction and valence bands, contains one hole trap acting as a recombination center and three types of electron traps representing shallow traps (level 1), 'dosimetric' traps (level 2) and deep traps (level 3). The 'dosimetric' traps are those that yield the luminescence signal to be used in dosimetry. Figure 1(a) represents those electronic transitions occurring during the irradiation stage, in which the dominant process is radiation-induced creation of electron–hole pairs and filling of traps. Figure 1(b) represents the equivalent transitions during the readout stage, in which the dominant process is the escape of electrons from traps by thermal or optical stimulation followed by recombination. The distinction between the irradiation and readout stages is obviously an oversimplification, because the processes could take place during either stage. In particular, the dosimeters can be intentionally stimulated during irradiation. Note that luminescence is also produced during irradiation due to electron–hole pair recombination.

The trapped charges can be released to the conduction or valence band using thermal or optical stimulation. In the case of optical stimulation, the escape probability p is the product of the photon flux ϕ (photons per unit time per unit area) and the photoionization cross-section σ, which describes the likelihood of a photon with energy $h\nu$ interacting with a particular defect (Bøtter-Jensen *et al* 2003):

$$p = \sigma\phi. \tag{1}$$

Once the trapped charges escape, electron–hole recombination is possible and the resulting luminescence is called TL or OSL depending on the stimulation process. The total TL or OSL

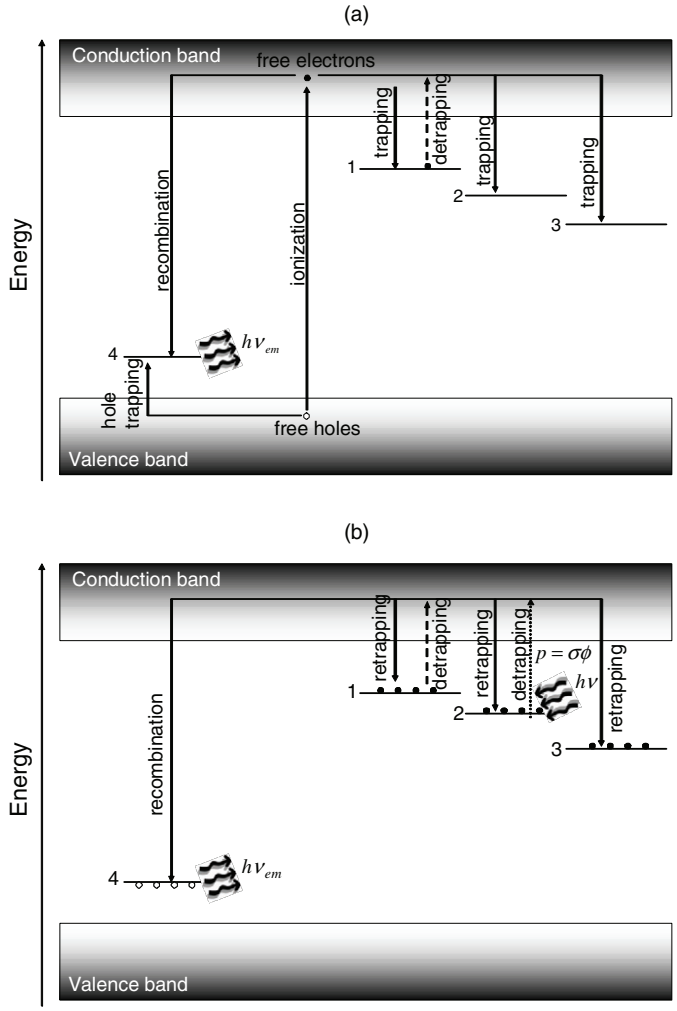

Figure 1. Possible electronic transitions between the dosimeter's energy levels during (a) irradiation and (b) readout stages.

associated with a particular trapping level is proportional to the trapped charge concentration and, ideally, to the absorbed dose of radiation.

The simplest, first-order model for TL and OSL processes assumes the absence of retrapping, i.e., all charges escaping from the traps recombine immediately producing luminescence. Therefore, the luminescence intensity is simply proportional to the variation in the trapped charge concentration given by

$$\frac{\mathrm{d}n}{\mathrm{d}t} = -np \tag{2}$$

where $n = n(t)$ is the trapped charge concentration at time t.

If the OSL readout is done by simply illuminating the dosimeter continuously with light of appropriate wavelength (McKeever 2001, Bøtter-Jensen *et al* 2003), the shape of the

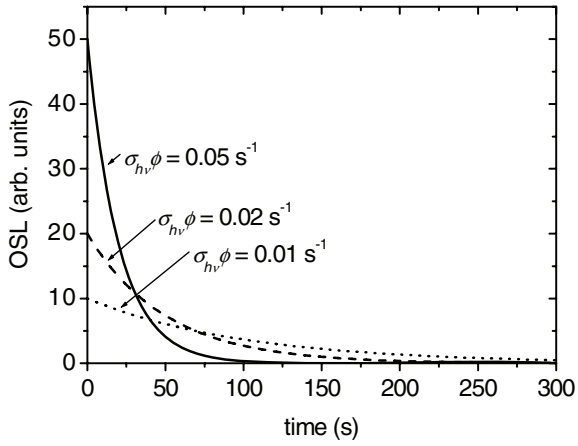

Figure 2. OSL intensity versus stimulation time for various light intensities, i.e., various values of $\sigma_{h\nu}\phi$, where $\sigma_{h\nu}$ is the photoionization cross-section and ϕ is the stimulation photon flux.

curve of OSL intensity versus stimulation time, the OSL curve, can be obtained by solving equation (2) using the probability (1) and a constant stimulation intensity ϕ:

$$I_{\mathrm{OSL}}(t) \propto n_0 \sigma \phi \, \mathrm{e}^{-\sigma \phi t}. \tag{3}$$

Because the escape probability is constant, the OSL intensity is an exponential decay following the trapped charge concentration. In a real dosimeter, the contribution from different trapping levels appears as a superposition of exponential decays.

Figure 2 illustrates the OSL curves for different stimulation intensities. For a photon flux (stimulation intensity) ϕ such that the probability $p = \sigma\phi = 0.05\ \mathrm{s}^{-1}$, the initial OSL intensity is higher and decays faster than an OSL curve obtained with a lower stimulation intensity ($p = \sigma\phi = 0.01\ \mathrm{s}^{-1}$). Integration of equation (3) leads to $\int I_{\mathrm{OSL}}(t)\,\mathrm{d}t \propto n_0$, from which one can see that the integrated OSL signal is proportional to the initial trapped charge concentration n_0 (i.e., to the absorbed dose of radiation) and is independent of the stimulation power. The initial OSL intensity is proportional to both n_0 (i.e., to the absorbed dose of radiation) and the photon flux ϕ (i.e., the stimulation power).

It is important to keep these observations in mind in OSL dosimetry. Some OSL readers allow the user to record the whole OSL curve and, therefore, choose between using the total OSL signal or parts of the OSL curve (such as initial OSL intensity) for dosimetry. Other readers stimulate the dosimeters for a short time, therefore recording just the equivalent to the initial OSL intensity.

In real materials, a purely exponential decay is rarely observed. Factors that can affect the OSL curve shape and/or the total OSL signal include the following:

(a) trapping at competing traps (deep and shallow);
(b) thermal stimulation of trapped charges from shallow traps;
(c) retrapping at the dosimetric trap;
(d) simultaneous stimulation from multiple trapping levels;
(e) recombination at multiple recombination centers;
(f) photo-transfer of charges from deep to the dosimetric and shallow energy levels.

In fact, the OSL decay curve is the result of a dynamic process that can be affected by the concentration of competitors represented by shallow and deep traps, the extent to which they

are occupied and the level of the absorbed dose. These factors in turn result in a dependence on the ionization density created by the radiation field in the crystal (Yukihara *et al* 2004, Yukihara and McKeever 2006a). Some of the processes and events relevant to the final character and properties of the OSL signal are outlined in the following section.

2.2. Key processes

Although it is beyond the scope of this review to discuss all possible processes affecting the OSL signal, in this section several are described which are particularly relevant to an understanding of recent results in the literature concerning applications in medicine.

2.2.1. Charge capture by shallow traps. Shallow traps are localized energy levels close to the edge of the conduction band in the case of electron traps (represented in figure 1 by level 1), or close to the valence band in the case of hole traps. 'Close' in this context means that the energy difference between the trap and the delocalized band is such that the escape probability for charges trapped in shallow traps is significant even at room temperature; consequently, the charge concentration in these energy levels can decrease over time scales ranging from minutes to days.

Shallow traps are generally associated with two important phenomena: phosphorescence observed immediately after irradiation and an initial increase in the intensity of the OSL signal upon stimulation.

The phosphorescence is caused by the recombination of charges escaping from the shallow traps following the end of the irradiation period. To avoid its influence in the OSL readout, it may be necessary to introduce a delay between dosimeter irradiation and readout to allow for the decay of the phosphorescence signal. Phosphorescence can also be observed immediately after optical stimulation due to charges stimulated from the dosimetric trap and captured by the shallow trap, resulting in a long 'tail' in the OSL signal.

The initial increase in the OSL curve is related to competition by shallow traps. At the beginning of the OSL readout, the shallow traps are empty and can capture charges escaping from the main dosimetric trap that would otherwise recombine. As a result, the overall OSL intensity is smaller than would be expected. However, as the shallow traps are filled and the number of charges captured by the shallow traps equals the number of charges escaping from them, the competition process becomes less important and the OSL intensity increases. Figure 3 illustrates the effect of shallow and deep traps on the OSL curves.

2.2.2. Charge capture by deep traps. Deep electron trap (level 3 in figure 1) and deep hole traps (not represented in the model depicted in figure 1) can act as competitors during the irradiation and readout stages, capturing charges released to the conduction and valence bands. As deep traps are filled, the sensitivity of the crystal can either increase or decrease, depending on the nature of the deep trap (Yukihara *et al* 2003, 2004, Yukihara and McKeever 2006a), but the overall effect is to introduce an undesirable dependence of the OSLD sensitivity on the irradiation history. For example, the deep electron trap depicted in figure 1 can capture charges released from the dosimetric trap, therefore decreasing the overall intensity of the OSL signal. This effect is illustrated in figure 3. However, as the deep traps are filled, becoming less competitive for the capture of charges, more electrons are available for recombination. This results in an effective increase in the sensitivity of the dosimeter. In some cases it is possible to reset the sensitivity by annealing the dosimeter at an appropriate temperature to empty the deep traps. In the case of Al_2O_3:C, an annealing at 900 °C for 15 min is recommended for both TL and OSL (Akselrod and Gorelova 1993, Yukihara *et al* 2003, 2004).

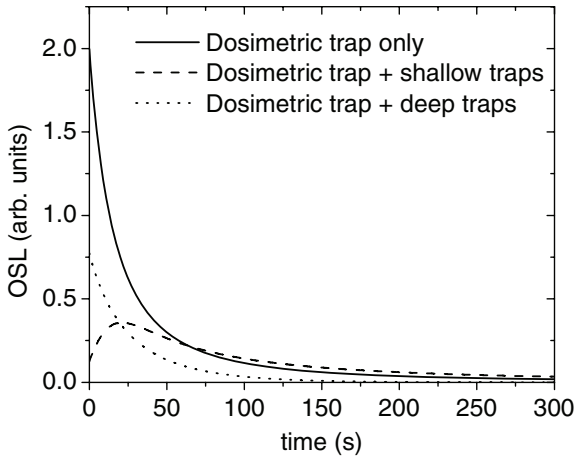

Figure 3. Theoretical OSL curves for a model containing only a dosimetric trap and recombination center or containing in addition shallow traps or deep traps. The curves were calculated using rate equations to describe the traffic of charges between different trapping levels and recombination centers in the dosimeter, as discussed by McKeever *et al* (1997).

2.2.3. Prompt recombination. Radioluminescence (RL) is produced by prompt electron–hole pair recombination during irradiation. In principle, the RL intensity is proportional to the rate of creation of electron–hole pairs and, therefore, it can be used to determine the dose rate. However, the RL intensity is also affected by the complex dynamic of trap filling in the crystal, since trapping is a process competing with recombination. As an example of the dynamic interplay between these competing processes, the reader is referred to the numerical calculations by Polf *et al* (2004) explaining the RL signal of Al_2O_3:C optical fibers subjected to simultaneous irradiation and stimulation. Therefore, the RL sensitivity may not be constant with the dose and corrections have to be implemented to take this effect into account.

2.2.4. Induction of signal by light. OSL can be induced by UV light by two mechanisms: direct ionization of defects and phototransfer of charges from deep traps. In a wide band-gap semiconductor or insulator, the ionization of atoms of the crystal requires photon energies higher than the band gap energy and, therefore, this process can usually be neglected. However, the ionization of defects can occur at photon energies lower than the band gap energy, as in the case of the ionization of F-centers in Al_2O_3, which requires photon energies of the order of 6 eV, as compared to a band gap of 9 eV (Evans *et al* 1994). The photoionization of defects creates free charges that can be trapped, producing TL and OSL in a similar way as ionizing radiation. In the case of dosimeters previously irradiated, UV can also transfer charges from deep traps to the dosimetric trap, resulting in the so-called phototransferred TL or OSL. For these reasons, it is important to protect the dosimeters from light even before irradiation, depending on the dose level to be measured.

2.3. Stimulation modalities

Because of the high degree of control in the stimulation that can be achieved with light sources, a variety of stimulation modalities have been proposed over the years.

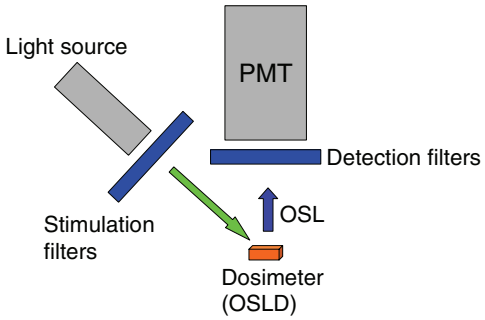

Figure 4. Main elements required in the design of an OSL reader.

2.3.1. Continuous-wave OSL (CW-OSL). Because of its simplicity, CW-OSL is the recommended stimulation modality for most applications. CW-OSL consists of the continuous illumination of the dosimeters while monitoring the OSL intensity. The CW-OSL curve is typically a decay curve as shown in figure 2.

2.3.2. Pulsed OSL (POSL). POSL is a useful technique for dosimetry of low doses. The technique consists in stimulating the dosimeter with bursts of short pulses of light from LEDs or lasers, while asynchronously monitoring the luminescence (Sanderson and Clark 1994). The pulse frequency is usually high, or of the order of hundreds or thousands of hertz, and the OSL signal detected in-between the pulses is integrated over many pulses. In dosimeters having luminescence centers characterized by long luminescence lifetimes, an appropriate choice of timing parameters allows the detection of most of the OSL signals while suppressing the counts associated with the scattered stimulation light, thereby improving the signal-to-noise ratios and the limits of detection (McKeever *et al* 1996, Akselrod and McKeever 1999). If the stimulation is carried out for a long time, a decay curve is observed similar to that shown in figure 2.

2.3.3. Other stimulation modalities. Linear modulation OSL (LM-OSL) was proposed by Bulur (1996) and consists of ramping the stimulation intensity linearly while monitoring the OSL intensity. The predicted shape of the LM-OSL curves increases linearly with the stimulation intensity, reaches a peak and decreases for further illumination times due to depletion of the traps. However, the LM-OSL technique has not been shown to provide any advantage over regular CW-OSL in dosimetry. Other time-varying stimulation modalities (exponential, sinusoidal, polynomial) are also possible but, as with LM-OSL, none of them have yet been shown to have particular utility in dosimetry.

2.4. Basic experimental setup

The essential elements required for an OSL measurement are represented schematically in figure 4 and include (i) a light source to be used for stimulation (e.g., a lamp, LED or laser); (ii) filters to select the wavelength of the light source and/or remove short-wavelength components; (iii) detection filters to block the stimulation light, while transmitting the OSL from the dosimeter; (iv) a light detector such as a PMT for registering the low light levels and (v) associated electronics (not shown in the figure).

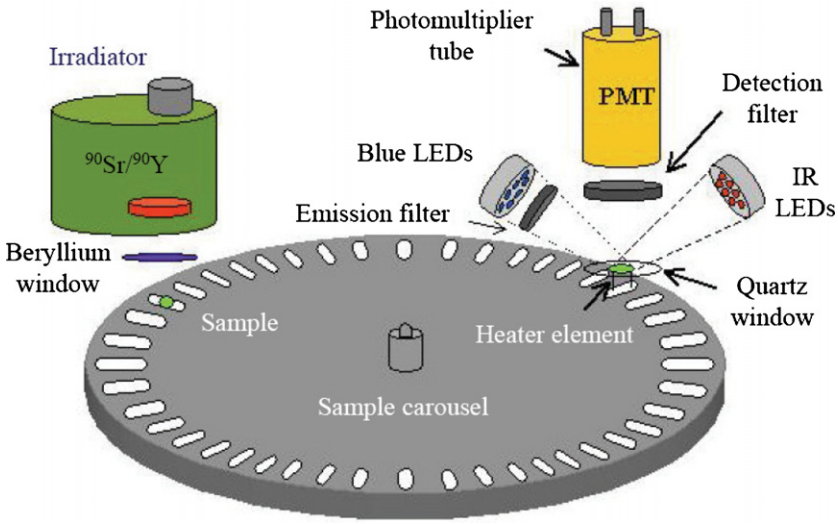

Figure 5. Schematic drawing of the Risø TL/OSL luminescence reader (courtesy of Risø National Laboratory, Denmark).

Because the intensity of the stimulation light is many orders of magnitude higher than the OSL signal, it is important to carefully choose the filters used in front of the stimulation light source and in front of the PMT to keep the stimulation light from being scattered into the PMT. As an example, when using broadband stimulation such as green (e.g., 525 nm) or blue (e.g., 470 nm) LEDs, long-pass filters such as Schott GG-420 or GG-475 can be used in front of the LEDs, while bandpass filters such as Hoya U-340 are used in front of the PMT (transmission between 290 nm and 370 nm) (Bøtter-Jensen *et al* 2003). In addition, if light such as the 532 nm line from a frequency-doubled Nd:YAG laser is used for stimulation, additional laser mirrors specifically designed to block the laser line can be placed in front of the PMT to reduce the background. For optimal sensitivity, the choice of filters has to take into account the OSL emission spectrum of the dosimeter and the spectrum of the light source.

2.5. Available OSL readers

2.5.1. Research OSL readers. High-capacity automated OSL readers have been introduced during the past decade (Bøtter-Jensen 1997). They are widely used in research and luminescence dating, being capable of performing sequences of TL measurements, OSL measurements and irradiations using a $^{90}Sr/^{90}Y$ beta source incorporated in the equipment. A typical schematic layout is shown for the TL/OSL reader produced by Risø National Laboratory in figure 5. Such readers are normally equipped with an array of blue and IR LEDs for stimulation, but green LEDs can be used. For dosimetry applications with Al_2O_3:C, green stimulation is currently recommended.

2.5.2. Landauer's OSL readers. Landauer's Luxel^{TM} badges are read out by the company using POSL systems similar to that described by Akselrod and McKeever (1999). The OSL is stimulated using the 532 nm line from a pulsed laser (frequency-doubled Nd:YAG) for a short period of time, while the OSL is measured in-between the laser pulses. Depending on the dose level, the dosimeter is read out using either a weak or strong beam, resulting in a large

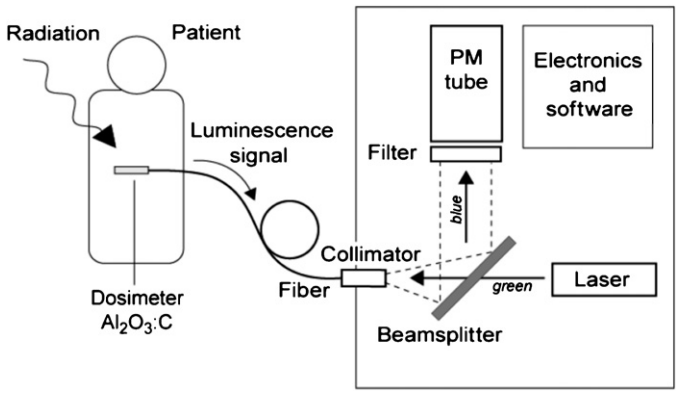

Figure 6. Conceptual diagram of the optical fiber systems developed by the research group at Risø National Laboratory (Aznar *et al* 2004), reproduced with permission of the author and IOP Publishing Ltd.

dynamic range (∼10 μSv–10 Sv). Laser mirrors and Corning 5–58 filters are used in front of the PMT to block the stimulation light.

InLight^{TM} OSL readers are manual or automatic readers recently introduced by Landauer Inc. and designed exclusively for use with Al_2O_3:C InLight^{TM} System dosimeters. They include a portable version, the microStar^{TM} reader. The OSL is read with a short stimulation (1 s) using an array of 38 green LEDs operating in the CW-OSL mode (Perks *et al* 2007). Depending on the dose level, two beam intensities are possible: for low doses, all 38 LEDs are used resulting in maximum stimulation and higher OSL signal, but also larger degree of signal depletion; for high doses, only 6 LEDs are used, resulting in a lower OSL signal, but low degree of signal depletion, ∼0.05% per readout (Jursinic 2007). The light detection system includes a PMT tube with Hoya B-370 filters in front of the PMT.

Landuaer also employs a custom-made reader for OSL strips designed for use in CT dosimetry. This reader uses a laser for stimulation and allows illumination of areas as small as 0.1 mm to obtain a dose profile along the length of the OSL strip.

2.5.3. Optical fiber systems. The concept of combining OSL probes with optical fiber systems is to use the optical fiber to deliver the stimulation light to the OSL probe and carry back the luminescence signal from the probe to the reader. The motivation for this approach, as opposed to a simpler scintillator probe, is (i) the possibility of obtaining two estimates of the absorbed dose, the first based on the RL signal emitted during irradiation and a second based on the OSL signal measured after irradiation and (ii) the possibility of separating the OSL signal originating from a single probe from other undesirable luminescence signals originated elsewhere (e.g., RL and Cerenkov light from the optical fiber itself—the so-called stem effect).

Figure 6 presents the schematics of the prototype optical fiber reader developed by the research group at the Risø National Laboratory (Andersen *et al* 2003, Aznar *et al* 2004). In this system a small Al_2O_3:C crystal is optically coupled to one end of an optical fiber, while the other end of the fiber is connected to a reader containing a stimulation source and a detection system. Light from a green laser is optically coupled to the optical fiber for the OSL measurements. The RL and OSL signals from the probes are carried by the fiber and reflected by the dichroic mirror to the PMT. Filters are used in front of the PMT to block the scattered

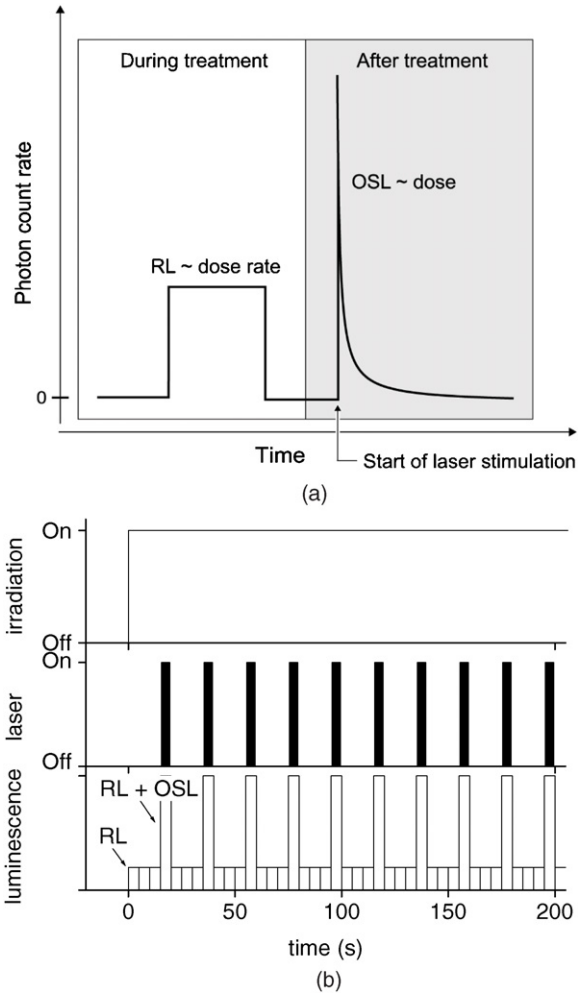

Figure 7. (a) Illustration of the 'RL and post-irradiation OSL' approach, in which the radioluminescence is recorded during irradiation and the CW-OSL is recorded after the irradiation is over (Andersen *et al* 2003) and (b) the 'periodic OSL stimulation' approach, in which the probe is stimulated periodically during irradiation (Polf *et al* 2004).

stimulation light. An alternative approach is to use bifurcated optical fibers to separately carry the stimulation light and luminescence signal (Huston *et al* 2002, Polf *et al* 2002).

To take advantage of the OSL signal and properties of Al_2O_3:C, two readout schemes were proposed: the 'RL and post-irradiation OSL' (Andersen *et al* 2003, Aznar *et al* 2004) and the 'periodic OSL stimulation' (Gaza *et al* 2004). In the 'RL and post-irradiation OSL' scheme, the RL signal is recorded during irradiation and the CW-OSL signal is recorded after the irradiation, as illustrated in figure 7(a). The RL signal provides information on the dose rate and, upon integration, on the absorbed dose at the location of the probe. After the irradiation is over, the Al_2O_3:C probe is stimulated and the CW-OSL signal is recorded, providing a second, independent estimation of the absorbed dose. Due to changes in the RL sensitivity with the absorbed dose, an algorithm and appropriate calibration are necessary to obtain the correct

dose rate from the real-time RL signal (Andersen *et al* 2006). In the case of pulsed sources such as clinical linear accelerators, the stem effect can be eliminated by taking advantage of the long luminescence lifetime of Al_2O_3:C. This is accomplished by synchronizing the optical fiber reader with the linear accelerator and gating the PMT to detect only the luminescence in-between the radiation pulses (Andersen *et al* 2006).

In the 'periodic OSL stimulation' scheme, short pulses of light are delivered to the OSL probe during irradiation to stimulate the OSL signal (figure 7(b)). In-between the light pulses, the signal consists mostly of RL and stem effect; whereas during the light pulses the signal is a sum of the RL, stem effect and OSL (Gaza *et al* 2004, Polf *et al* 2004). The 'real-time OSL signal' can then be obtained by subtracting the PMT signal obtained in-between stimulation from the PMT signal obtained during stimulation.

The problem with the 'periodic OSL stimulation' is that each stimulation pulse depletes a fraction of the OSL signal (Polf *et al* 2004), therefore introducing the need for a correction algorithm. Mathematical approaches to implement this correction algorithm were investigated by Gaza *et al* (2005) with reproducibility of the order of 1–8% for an optical fiber dosimeter using Al_2O_3:C probes, but the algorithm has not been tested in clinical situations. A second disadvantage of the 'periodic OSL stimulation' approach is that, because the probe is being stimulated during irradiation, the net OSL signal is not preserved to estimate the absorbed dose after the irradiation is over.

We should also mention the work by Gaza and McKeever (2006) and Klein and McKeever (2007) on optical fiber systems using KBr:Eu probes for real-time dosimetry. Although these probes are not tissue equivalent and fade at room temperature, the OSL can be stimulated very quickly, the whole OSL decay being recorded within tens of millisecond using a stimulation power of 20 mW at 658 nm. In this case, each stimulation pulse generates a complete OSL curve from which the absorbed dose accumulated since the last stimulation pulse can be obtained.

It can be seen that the implementation of the readout procedures required to take advantage of the OSL probes is complicated. The main problems encountered are the changes in the RL and OSL sensitivities with dose due to filling of deep traps that act as competitors (Polf *et al* 2004, Andersen *et al* 2006, Damkjær *et al* 2007) and the temperature dependence due to shallow traps (Edmund and Andersen 2007, Damkjær *et al* 2007). Although some OSL probes have been used in a clinical setting, the research is still under development.

2.6. *Basic properties of Al_2O_3:C*

Al_2O_3:C is grown in reducing conditions in the presence of carbon, creating a relatively high oxygen vacancy concentration and defects known as F- and F^+-centers (oxygen vacancies with captured electrons). The F^+-center concentration is of the order of 10^{15}–10^{16} cm^{-3} and the F-center concentration is of the order of 10^{17} cm^{-3} (Akselrod *et al* 1990, McKeever *et al* 1999). The OSL sensitivity of the crystal is correlated with the concentration of F^+-centers, which act as recombination centers (McKeever *et al* 1999).

One of the attractive features of Al_2O_3:C is the fact that there is a dominant trapping level responsible for the TL and OSL, the TL peak occurring at ∼470 K (∼200 °C) depending on the heating rate (figure 8(a)). This suggests that the OSL signal (figure 8(b)) is stable at room temperature, and indeed room temperature fading is not appreciable over a period of up to 85 days, at least for personal dosimetry applications (Bøtter-Jensen *et al* 1997).

The dominant emission band in Al_2O_3:C is a broadband centered at 420 nm attributed to F-center luminescence (Lee and Crawford Jr 1979, Akselrod *et al* 1990, Markey *et al* 1995). In the proposed mechanism for the OSL process, electrons are optically released from

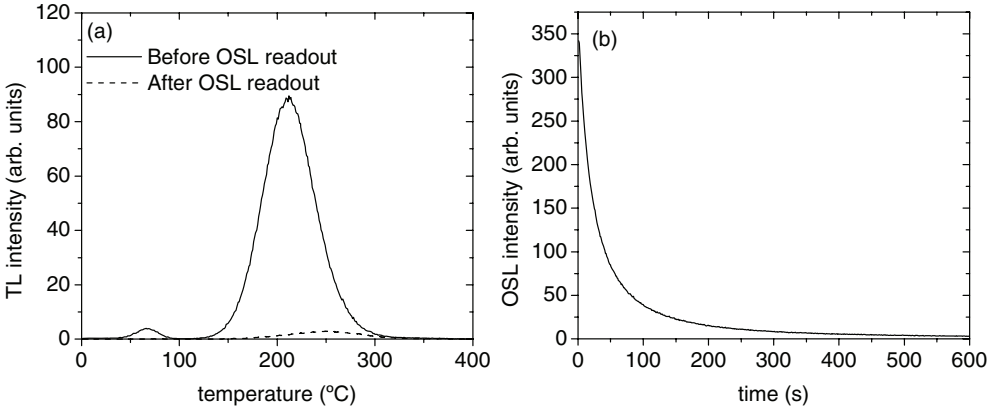

Figure 8. (a) TL measurement of irradiated Al_2O_3:C powder before and after OSL readout, at a heating rate of 5 °C s^{-1} and (b) green-stimulated OSL measurement of irradiated Al_2O_3:C powder. The TL and OSL measurements were carried out using a Risø TL/OSL-DA-15 reader with Hoya U-340 filters in front of the PMT. The Al_2O_3:C powder in these measurements is the same one used in the manufacturing of the Luxel^{TM} dosimeters (Landauer Inc.).

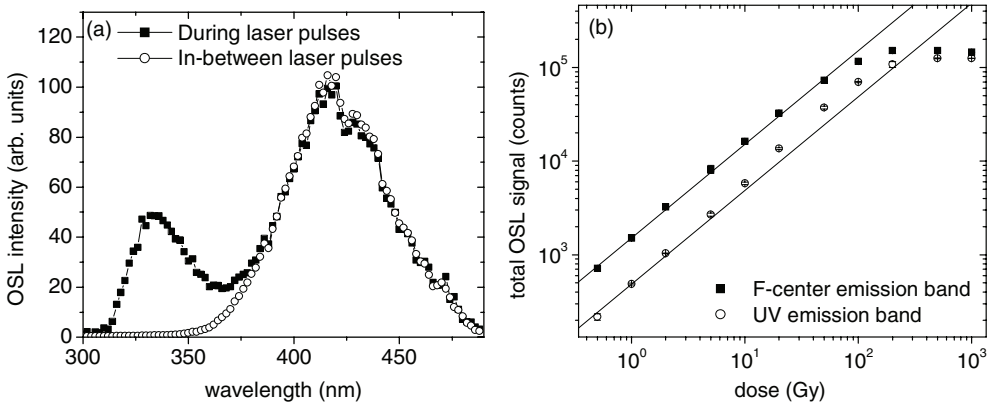

Figure 9. (a) Al_2O_3:C OSL emission spectrum during an in-between laser pulses and (b) dose response of the UV and F-center emission bands (Yukihara and McKeever 2006b).

trapping centers, recombining with F^+-centers. The recombination process creates excited F-centers which relax radiatively producing the observed luminescence. Figure 9(a) shows that an UV emission band at 334 nm can also be observed (Yukihara and McKeever 2006b), but its contribution is only significant in special circumstances (e.g., using Hoya U-340 filters in front of the PMT, which block most of the F-center emission but transmit the UV emission band).

For general applications, the OSL response of Al_2O_3:C can be considered to be approximately linear over a wide range of doses, up to ∼50 Gy if only the main luminescence band is detected (Yukihara and McKeever 2006b). The UV emission band shows supralinearity starting at 10 Gy (figure 9(b)). Sublinearity occurs for doses above 100 Gy.

In spite of these apparently simple properties, studies suggest that the main TL peak is actually composed of trapping centers with a distribution of activation energies and

photoionization cross-sections (Akselrod and Akselrod 2002, Whitley and McKeever 2001). In addition, there is also the presence of a small TL peak at low temperatures (figure 8(a)), indicating the presence of shallow traps which introduce a temperature dependence on the Al_2O_3:C OSL signal (Edmund and Andersen 2007, McKeever *et al* 1997). The presence of deep traps can also be inferred from TL measurements (Molnar *et al* 2002) or step-annealing procedures in which the TL/OSL sensitivity and recombination center concentration are monitored (Yukihara *et al* 2003, 2004). A model for the Al_2O_3:C that explains some of the effects due to deep traps is discussed by Yukihara and McKeever (2006a). Pagonis and colleagues carried out detailed calculations to show that this model explains the Al_2O_3:C dose response (Pagonis *et al* 2006).

Besides the light sensitivity, one of the disadvantages of Al_2O_3:C is the effective atomic number of 11.28 (Bos 2001), which causes an overresponse to low-energy x-rays (Akselrod *et al* 1990, Mobit *et al* 2006).

2.7. Available Al_2O_3:C dosimeters

The only Al_2O_3:C dosimeters commercially produced today are those produced by Landauer Inc. and used in the Luxel™ and InLight™ systems. Some researchers still have access to single crystals produced at the Urals Polytechnic Institute (Russia) in the 1990s (Akselrod *et al* 1990), some of which were commercialized by Harshaw under the trade name TLD-500. The following is a brief description of the many forms in which Al_2O_3:C can be found.

2.7.1. Single crystals. These dosimeters are typically 5 mm in diameter and 0.9 mm in thickness. Because of the mass (∼70 mg) and high sensitivity, they are excellent for low dose measurements. Another advantage is that they can be annealed (e.g., 900 °C for 15 min) to empty deep electron and hole traps and can be re-used almost indefinitely. The disadvantage is the large dosimeter-to-dosimeter variability, caused by the fact that each crystal can have slightly different defect concentrations. Consequently, the OSL intensity, OSL curve shape and dose response can vary from dosimeter to dosimeter, requiring individual chip calibration for careful dosimetry.

2.7.2. Dosimeters from Landuaer Inc. The dosimeters used by Landuaer Inc. are produced using Al_2O_3:C crystals grown by Landauer Stillwater Crystal Growth Division. The crystals are converted into powder and used to produce long plastic tapes with a total thickness of 0.3 mm, from which dosimeters of the desired shape and size can be obtained for use in Landauer's various dosimeter systems. The dosimeters in Landuaer's Luxel™ badges are approximately 1.7 cm × 2.0 cm. InLight™ badges (cartridges) contain four round dosimeters 7.0 mm in diameter that can be read individually (Perks *et al* 2007). The InLight™ Dot dosimeters contain a single round dosimeter 7.0 mm in diameter that can be placed in an adapter for readout in the InLight™ or microStar™ reader. Long strips (OSL strip) are also being used to determine the dose profiles in computed tomography. Because these dosimeters are produced from the same type of tape, their intrinsic properties are identical. However, the results may vary with reader and readout protocol.

The advantage of these dosimeters is the uniformity in sensitivity and properties, because the Al_2O_3:C powder used in the production is a homogenized mixture of different crystal growth runs. The disadvantage is that they cannot be annealed to high temperatures as in the case of the single crystals because of the plastic. Although the OSL signal can still be erased by optical illumination (bleaching), sensitivity changes related to filling of deep traps in the crystal cannot be reversed.

2.7.3. Microcrystals and optical fibers. Smaller crystals have also been produced in an experimental scale for use as optical fiber probes by either cutting single crystals into smaller pieces, e.g. 0.5 mm × 0.5 mm × 4 mm (Edmund *et al* 2006), or using alternative growth processes (Bloom *et al* 2003). Because Al_2O_3 is a hard and inert material, small crystals would also be of interest for *in vivo* dosimetry in radiobiology experiments. This possibility has yet to be explored.

2.8. Other materials

BeO has already been investigated for dosimetry because of its sensitivity, easy access and low effective atomic number ($Z_{\text{eff}} = 7.21$) (Bos 2001). Bulur and Göksu (1998) carried out a detailed investigation of the OSL properties of BeO ceramics (Thermalox™, Brush Wellman Inc., USA) and determined that the main OSL signal is related to traps that become unstable at a temperature near 340 °C and have an activation energy of ∼1.7 eV. However, the BeO TL curve and temperature studies also showed evidence of a shallow trap in addition to the main trapping center (Bulur and Göksu 1998). The luminescence spectrum of BeO Thermalox™ 995 is a wide emission from 250 to 500 nm, peaking at ∼325 nm (McKeever *et al* 1995). The luminescence shows thermal quenching for relatively low temperatures, in the range from 50 to 120 °C, introducing a dependence of the OSL signal on the readout temperature (Bulur and Göksu 1998).

Sommer and Henniger (2006) and Sommer *et al* (2007) showed that the BeO response is linear over almost six decades and reproducible within 5% independent of thermal annealing. The authors reported a minimum detectable dose of ∼1 μGy. The signal showed an initial fading of 6% in the first few hours but remained at ∼1% in the next six months. The energy response shows an under-response to low-energy photons. The authors argue that BeO should provide high resolution in imaging applications because of its strong optical attenuation.

One problem that has plagued many new materials is the presence of shallow traps contributing to the OSL signal, which causes fading over a variety of time scales. For example, Bos *et al* (2006) reported results on MgO:Tb^{3+}, the TL for which shows high-temperature peaks that can be stimulated with IR and green light. The dose response is linear up to 10 Gy, but the signal showed considerable fading (43%) after 36 h. Yoshimura and Yukihara (2006) also surveyed the OSL of a range of materials, including Mg_2SiO_4:Tb, Al_2O_3:Cr,Mg,Fe, barium aluminoborate glasses and $MgAl_2O_4$ spinels. In spite of the sometimes intense OSL signal, all materials exhibit fading to different degrees.

2.9. Other practical aspects in OSL dosimetry

2.9.1. Initial OSL intensity versus total OSL signal. As long as the OSL decay curve shape is independent of the dose, it is irrelevant whether one uses the initial OSL intensity or the total OSL signal in dosimetry—except for the fact that the initial OSL intensity is more susceptible to fluctuations in stimulation power (see section 2.1). However, changes in the Al_2O_3:C OSL curve shape have been observed for doses above ∼10 Gy (Yukihara *et al* 2004). This results in different dose response curves for the initial OSL intensity and total OSL signal, as shown in figure 10.

2.9.2. Possibility of re-estimation of the absorbed dose. Because of the Al_2O_3:C high sensitivity and precise control provided by the optical stimulation, the estimation of the absorbed doses in OSL dosimetry does not require stimulation of the dosimeter until the dosimetric traps are completely emptied; short stimulation times of the order of 1 s or even

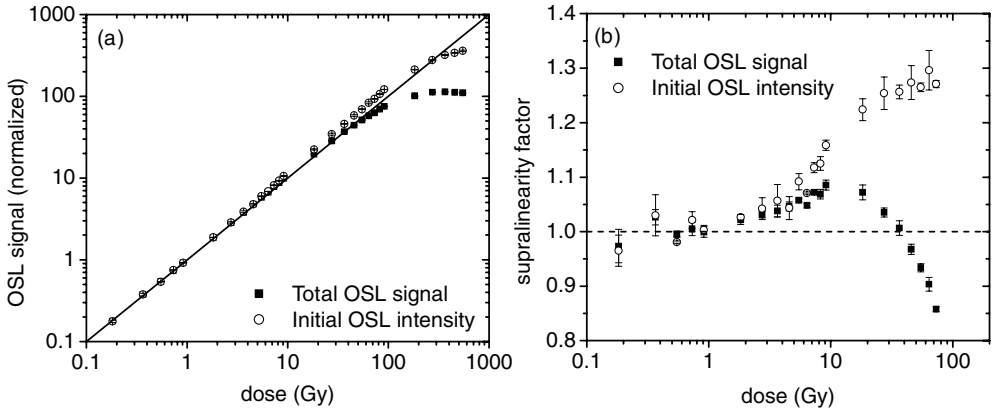

Figure 10. (a) Luxel^{TM} dose response for the initial OSL intensity and total OSL signal and (b) supralinearity factor calculated from the dose response. The initial OSL intensity corresponds to the first 1 s of stimulation, and the total OSL signal corresponds to the total OSL detected over 600 s of stimulation. The data were taken using a Risø TL/OSL-DA-15 reader with Hoya U-340 filters (7.5 mm total thickness) plus a 2 mm thick Schott WG-360 filter in front of the PMT, and the dosimeters were irradiated with the ^{90}Sr/^{90}Y beta source incorporated in the Risø reader, calibrated against a ^{60}Co gamma source in dose to water.

less can be sufficient. As a result, the radiation-induced trapped charge concentration can be preserved for future readouts. The signal depletion needs to be evaluated on a case-by-case basis, since it is dependent on the energy delivered to the dosimeter during stimulation.

2.9.3. Choice of optical filters. When choosing the optical filter to be used in front of the PMT or comparing results obtained using different OSL readers, it is important to keep in mind the dosimeter's emission spectrum. In the case of Al_2O_3:C, the emission is dominated by the F-center band centered at 420 nm, but the smaller UV emission band observed at 335 nm can affect the results depending on the detection filters and the stimulation mode. For example, using CW-OSL and Hoya U-340 filters in front of the PMT, the UV emission band contribution is approximately 20% of the F-center emission band contribution at low doses. However, the UV contribution increases at high doses or high LET radiation, becoming comparable to the F-center contribution (Yukihara *et al* 2006). In the case of the POSL technique, only the F-center is detected because of its long lifetime; the UV center does not contribute to the OSL signal in-between the stimulation pulses because of its short lifetime (Yukihara and McKeever 2006b). Figure 11 shows the Al_2O_3:C emission spectrum typical for low-medium doses and the transmission of various optical filters commonly used in OSL dosimetry of Al_2O_3:C.

3. Applications

3.1. Radiotherapy

There are a few investigations on the characterization of Al_2O_3:C OSLDs for clinical dosimetric measurements of high-energy photon and electron beams using different types of readers, phantoms and methodologies. A consistent picture has started to emerge regarding some of the generalizable aspects related to the application of Al_2O_3:C OSLDs in radiotherapy, whereas other aspects seem to depend on the particularity of each study. For quick reference,

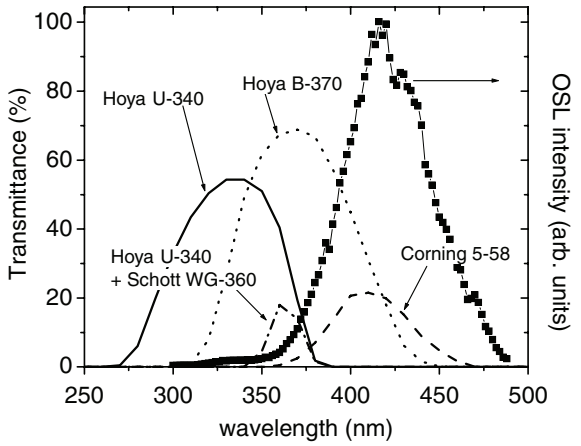

Figure 11. Comparison between the Al_2O_3:C emission spectrum during a CW-OSL readout, calculated from data from Yukihara and McKeever (2006b), and optical transmission of various filters used in several studies: Hoya U-340 (Yukihara *et al* 2004), Corning 5-58 or equivalent filter (Marckmann *et al* 2006, Edmund *et al* 2007, Damkjær *et al* 2007, Edmund and Andersen 2007, Andersen *et al* 2006), Hoya B-370 (Jursinic 2007) and a combination of Hoya U-340 and WG-360 filter (Yukihara *et al* 2005, 2007). The transmittance was calculated for typical thicknesses and may vary from equipment to equipment. See the cited references for details.

Table 1. OSL studies of interest for dosimetry in radiotherapy and respective types of OSLDs, readers and protocols adopted.

Publication	Type of OSLD	Reader, optical filter	Protocol
(Andersen *et al* 2003, 2006, Aznar *et al* 2004, Edmund and Andersen 2007)	Al_2O_3:C single crystals	Optical fiber reader, 395°–440° nm bandpass filter	'RL and post-irradiation OSL'
(Jursinic 2007)	InLight™ Dot	microStar™, Hoya B-370	CW-OSL; initial OSL intensity
(Miller and Murphy 2007)	Luxel™	Custom-made, 390–450 nm bandpass filter	CW-OSL; initial OSL intensity
(Schembri and Heijmen 2007)	Luxel™	Landauer Inc., 380–440 nm bandpass filter	POSL; initial OSL intensity
(Yukihara *et al* 2005, 2007)	Luxel™	Risø TL/OSL reader, Hoya U-340 + Schott WG-360	CW-OSL; total OSL signal
(Viamonte *et al* 2008)	InLight™ Dot	microStar™, Hoya B-370	CW-OSL; initial OSL intensity

table 1 summarizes the main types of OSLDs, readers and protocols adopted by each study to be discussed in the following sections.

3.1.1. Precision of the technique. It is difficult to assess the final precision that could be achieved with the OSL technique, since it depends on the particular reader, dosimeter, readout protocol and analysis methodology. Counting statistics and reader stability are among the elements that contribute to the uncertainty in the OSL signal, whereas batch reproducibility can be a limiting factor if batch calibration is used. Due to the high sensitivity of Al_2O_3:C, counting statistics are generally not the dominant source of uncertainty in radiotherapy. The overall reader stability obviously depends on each particular instrument. In the case of the

microStar reader, random fluctuations are reported to be of the order of 1% (Viamonte *et al* 2008). For InLight Dot dosimeters irradiated with 0.5 Gy using a ^{60}Co source and readout using a microStar^{TM} reader, Viamonte *et al* (2008) reported a batch variability of 4.2% (1σ) for InLight Dot dosimeters irradiated with 0.5 Gy using a ^{60}Co source and readout using a microStar^{TM} reader, whereas Schembri and Heijmen (2007) reported a batch variability of the order of 1–3% for Luxel^{TM} dosimeters irradiated with doses up to 2 Gy of a 6 MV photon beam and sent to Landauer Inc. for readout.

Yukihara *et al* (2005) proposed a different methodology to achieve high precision in radiotherapy using the Risø TL/OSL reader without having to worry about dosimeter-to-dosimeter variability or changes in the reader sensitivity. The methodology consists in (i) measuring the original OSL signal S for a total stimulation period of 600 s; (ii) irradiating the dosimeters with a fixed dose using the ^{90}Sr/^{90}Y beta source incorporated in the Risø reader; (iii) measuring the OSL signal S_R due to a reference dose (0.96 Gy) and (iv) calculating the ratio S/S_R. Because the ratio S/S_R is obtained using the same dosimeter and reader, any dependence on the dosimeter or reader sensitivity is cancelled and the same value of S/S_R is obtained for all dosimeters, irrespective of the OSLD sensitivity or day of measurement (as long as the reference dose is constant). This methodology is not identical to individual calibration, because the reference dose value is not used in the calculations; individual calibration of the OSLDs is not straightforward because of the sensitivity changes caused by previous irradiation. In the proposed methodology, the calibration curve has to be determined using the same procedure described above, but irradiating a different set of dosimeters with known doses before step (a). The calibration curve consists of values of S/S_R as a function of the dose. The advantage is that no correction or strict control on the preparation of the dosimeters is necessary, and sensitivity changes (including those related to supralinearity) are automatically taken into account and corrected for.

Figure 12 illustrates the advantage of the 'S/S_R' methodology by comparing the distribution of 50 different dosimeters irradiated with 0.665 Gy in identical conditions. The standard deviation of the ratio S/S_R was only 0.7%. An uncertainty analysis demonstrated that this methodology allows the determination of the absorbed dose with a precision better than 1% up to 10 Gy for a single OSLD readout (Yukihara *et al* 2007).

The use of prototype optical fiber readers has also been demonstrated to enable precise absorbed dose estimates in photon and electron fields using Al_2O_3:C single-crystal probes. For example, Andersen *et al* (2003) demonstrated a short-term (38 h) reproducibility of 0.2%, which includes the variability due to the x-ray source used for the tests. Tests performed with 6 MV and 18 MV photon beams from a clinical linear accelerator lead to a conservative estimation of the reproducibility of 0.5% (Aznar *et al* 2004). Tests in an IMRT treatment simulation showed a difference of only 0.9% between the doses estimated using the OSL probes and the planned dose (Andersen *et al* 2006).

3.1.2. Dose response. The OSL dose response depends on the particular experimental parameters and the dosimeter type used. For Al_2O_3:C single crystals, the dose response can vary depending on the crystal growth (Yukihara *et al* 2004), on the optical filters used in front of the PMT (Yukihara and McKeever 2006b) and on the choice between the initial OSL intensity or total OSL signal (figure 10). Deviations from linearity are generally explained in terms of filling of deep electron and hole traps that compete for the capture of free charges during either irradiation or readout stage (Yukihara *et al* 2004), similar to the situation for TL (Yukihara *et al* 2003). Therefore, the dose response can also be influenced by the dose history of the dosimeter due to the filling of deep traps (Edmund *et al* 2006).

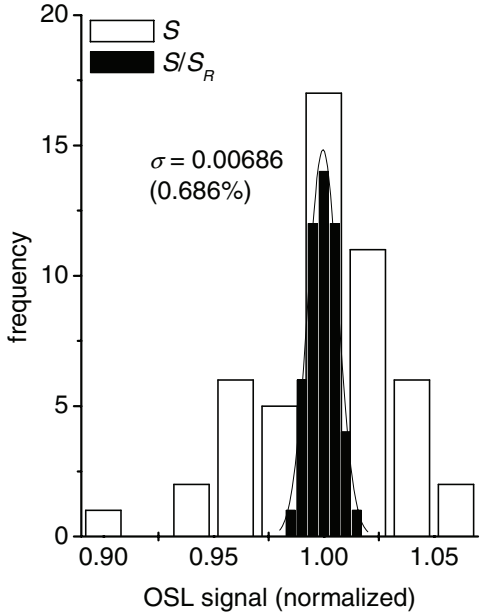

Figure 12. Distribution of the OSL signal S and ratio S/S_R for 50 dosimeters irradiated with the same dose using a 6 MV photon beam from a linear accelerator (Yukihara *et al* 2005), reproduced with permission from IOP Publishing Ltd.

Both Jursinic (2007) and Schembri and Heijmen (2007) reported a small supralinearity for doses from a 6 MV photon beam above around 2–Gy. Yukihara *et al* (2007) also noticed a small supralinearity for doses above ∼5 Gy using Luxel^{TM} dosimeters read using a Risø TL/OSL reader. These observations are consistent with the dose response presented in figure 10.

3.1.3. Sensitivity changes. The Al_2O_3:C OSL sensitivity changes with irradiation history due to the filling of deep electron and hole traps that act as competitors during irradiation and readout (Yukihara *et al* 2004), a phenomenon that is generally linked to supralinearity. The degree of sensitization may be small for personal dosimetry applications, but a sensitization of a few per cent is sufficient to introduce additional uncertainty for radiotherapy applications.

Jursinic (2007) monitored the OSL sensitivity of InLight^{TM} Dot dosimeters after sequences of bleaching, irradiation and readout, as a function of the total accumulated dose. According to the authors, the sensitivity was unchanged (within an experimental uncertainty of 0.6%) up to accumulated doses of 20 Gy, but it decreased for higher doses. These results seem to indicate the possibility of re-using the OSLDs, at least under similar experimental conditions. However, we should point out that the absence of sensitization is not consistent with the supralinearity observed by the same authors above ∼2 Gy. Figure 13 shows the result of an independent study in which the Luxel^{TM} dosimeters were irradiated with different doses from ∼0.01 to 60 Gy, bleached for several days and irradiated with a 0.91 Gy test dose to determine the OSL sensitivity. The graph in figure 13 shows the OSL sensitivity as a function of the previous dose received by the dosimeter. Note that the sensitivity increases in the same dose range corresponding to the onset of supralinearity (figure 10(b)).

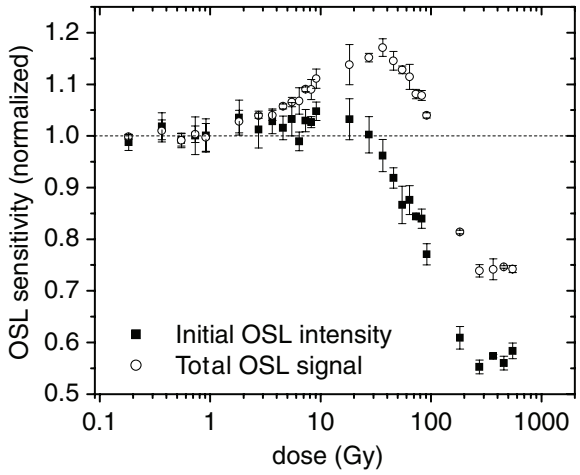

Figure 13. Luxel^{TM} OSL sensitivity as a function of the previous dose received by the dosimeter, determined by the OSL signal after long bleaching under fluorescent light for days and irradiation with a test dose (^{90}Sr/^{90}Y beta source) of 0.91 Gy. The initial OSL intensity corresponds to the first 1 s of stimulation, and the total OSL signal corresponds to the total OSL detected over 600 s of stimulation. The OSL readouts were performed using a Risø TL/OSL reader with Hoya U-340 and WG-360 filters in front of the PMT.

3.1.4. Dependence on beam quality. The dependence of the Al_2O_3:C OSL response has been tested for photon beams with energies between 6 MV and 18 MV, and for electron beams with energies between 6 MeV and 20 MeV. Jursinic (2007) did not observe significant variations within measurement uncertainties (0.9%) for the InLight^{TM} Dot dosimeters irradiated with 6 MV or 15 MV photons, and electron beams with energy between 6 and 20 MeV (figure 14(a)). This result is consistent with other reports in the literature (Viamonte *et al* 2008). Aznar *et al* (2004) reported a variation of 0.6% in output for both RL and OSL signals of Al_2O_3:C fiber probes irradiated with 6 MV or 18 MV photon beams (uncertainty of 0.5%). Andersen *et al* (2003) showed that the variation in response of Al_2O_3:C fiber probes for 18 MV photon beam and 20 MeV electron beam compared to 6 MV photon beam is less than 0.5% (uncertainty of 0.4%). Yukihara *et al* (2007) also investigated the Luxel^{TM} response for 6 MV and 18 MV photon beams, and electron beams with energy from 6 MeV to 20 MeV. After a fixed correction of 1.9% for the electron beam data, the response to all beam qualities was within $\pm$0.5%, with an uncertainty of 0.7% (figure 14(b)).

The variation in the beam energy with depth in water for either photons or electrons also did not seem to affect the determination of the depth–dose curves. Aznar *et al* (2004) obtained an agreement of 1% also between Al_2O_3:C fiber probes and p-doped Si diodes (Scanditronix/Wellhöfer). Yukihara *et al* (2007) compared OSLD depth–dose curves obtained using Luxel^{TM} and ionization chamber measurements for both photon and electron beams, obtaining an agreement within $\pm$1% or distance-to-agreement of the order of 0.5–1 mm.

At the moment, the only Monte Carlo investigation in the radiotherapy range was done by Mobit *et al* (2006) for a Al_2O_3:C chip modeled as a disc of 2.85 mm of diameter by 1 mm thickness. In their calculations, the difference in response between 25 MV and 6 MV photons is less than 2%, and varies by less than 3% when compared to a ^{60}Co gamma field.

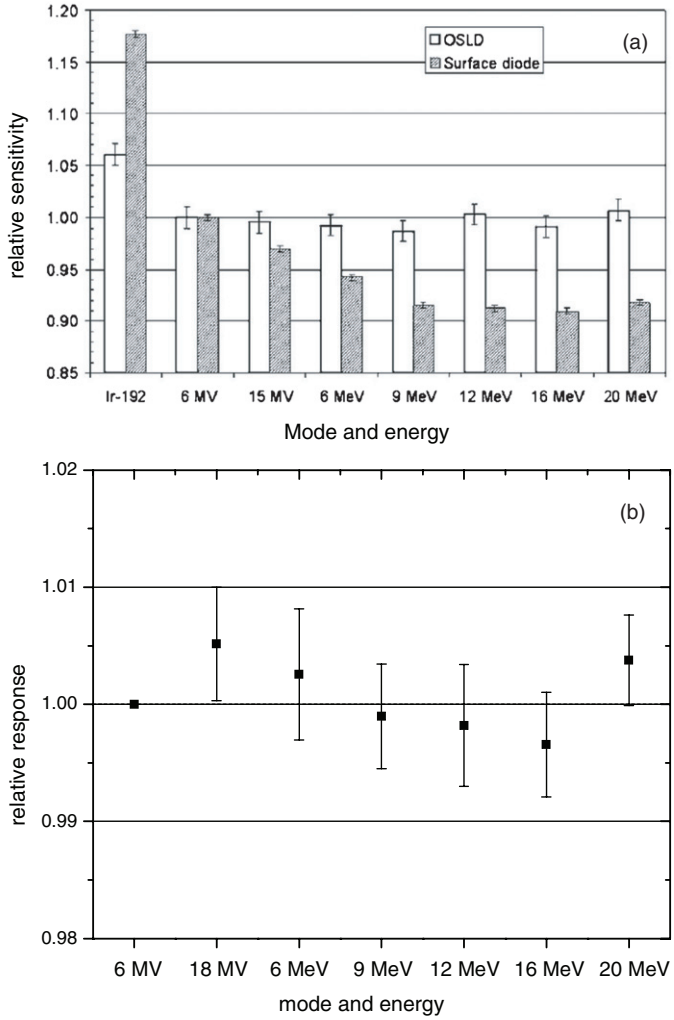

Figure 14. Dependence of OSLD sensitivity with beam quality for Ir-192 gamma rays (0.38 MeV), photon beams with energy between 6 MV and 18 MV photon beams, and electron beams with energy from 6 MeV to 20 MeV: (a) data from Jursinic (2007), reproduced with permission of the author and the American Association of Physicists in Medicine and (b) data from Yukihara *et al* (2007), which includes a fixed correction of 1.9% for the electron beam data.

3.1.5. Fading and transient signals. Jursinic (2007) followed the signal of three OSLDs irradiated with 1 Gy and observed a transient signal with a half-life of about 0.5–1 min (figure 15(a)). For the remainder of his study, Jursinic adopted an 8–15 min interval between irradiation and readout to allow for the decay of this transient component. The author also observed a decay of about 2% up to the maximum time investigated (2.5 days). A decay of 2–3% was also observed by Miller and Murphy (2007) for three dose levels (1 Gy, 10 Gy and 50 Gy), although the uncertainties associated with the data are between 0.8% and 2.2%.

This transient component observed in the first minutes after irradiation may be related to shallow traps. A higher and time-dependent OSL signal can be observed due to phosphorescence caused by shallow traps immediately after irradiation or due to the fact that

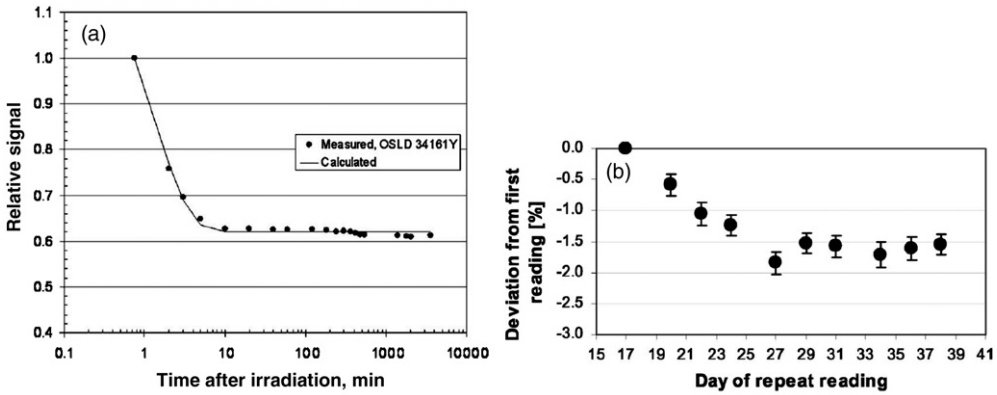

Figure 15. OSL intensity as a function of time elapsed since irradiation: (a) data from Jursinic (2007) for InLight™ Dot dosimeters readout using a microStar™ reader, reproduced with permission of the author and the American Association of Physicists in Medicine and (b) data from Schembri and Heijmen (2007) for Luxel™ dosimeters readout by Landauer Inc., reproduced with permission of the author and the American Association of Physicists in Medicine.

following irradiation the shallow traps are filled and, therefore, are not effective competitors for the capture of charges stimulated from the dosimetric trap. In either case, a strict correlation between this transient signal and shallow traps has not been demonstrated and the exact mechanism has not been established.

On a different time scale, Schembri and Heijmen (2007) compared the signal from 125 Luxel™ dosimeters irradiated with 2 Gy and sent to Landuaer Inc. for repeated readout after intervals ranging from 17 days to 38 days after irradiation. The dosimeter's average reading decreased by approximately 1.8%, reaching a stable value after approximately 27 days after irradiation (figure 15(b)).

The issue of OSL signal stability needs more detailed investigations in which the stability of the OSL readers used is taken into account.

3.1.6. Light sensitivity and bleaching. By definition OSLDs are sensitive to light and this sensitivity provides both advantages and disadvantages. On the one hand, there is the need to protect the OSLDs from unintentional light exposure following irradiation, which can prematurely deplete the OSL signal. On the other hand, there is the possibility of intentionally erasing prior radiation-induced signals in order to re-use the dosimeters. Jursinic (2007) investigated the OSL decay for different exposure periods for three light levels: 'dim room light', 'bright room light' and a '150 W tungsten-halogen light' used for bleaching the dosimeters. An important step in their investigation was the introduction of a 3 min delay between light exposure and dosimeter's readout, to avoid the influence of the shallow traps. (With light exposure, some of the freed charges can be captured by the shallow traps, contributing to phosphorescence.) Their results are presented in figure 16.

3.1.7. Temperature dependence. The dependence of the response of Al_2O_3:C Luxel™ OSLDs on the dosimeter temperature during irradiation was investigated by Jursinic (2007), Miller and Murphy (2007) and Yukihara *et al* (2007) using different readout equipment and protocols. Jursinic (2007) investigated the temperature dependence on the range from 10 °C to 40 °C using InLight™ Dot dosimeters and readout in a microStar™ reader. Within the

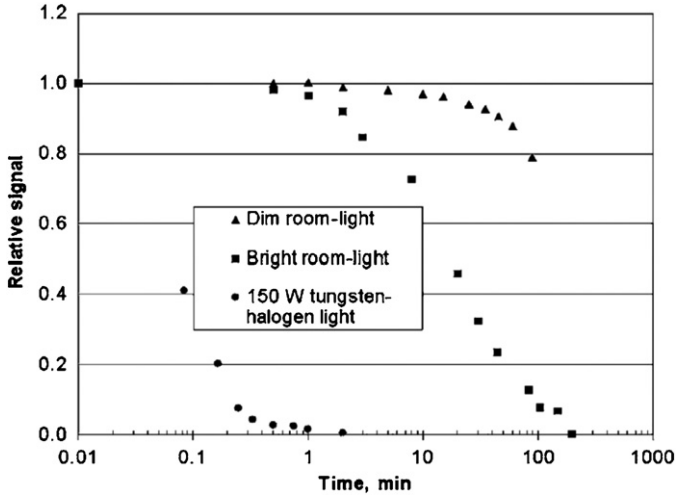

Figure 16. Effect of light exposure on Luxel™ OSL signal: (a) data from Jursinic (2007), reproduced with permission of the author and the American Association of Physicists in Medicine.

experimental uncertainties, the author did not observe any significant temperature dependence of the OSLD response. The data of Miller and Murphy (2007) indicate a 0.07% variation per degree Celsius, which would imply a variation of almost 1% between room and body temperatures. Yukihara *et al* (2007) examined the temperature dependence of the total OSL signal from Luxel™ dosimeters irradiated in the temperature range from 21 °C to 36 °C and read using a Risø TL/OSL-DA-15. The temperature dependence was not statistically significant within an uncertainty of 0.7%. These preliminary results show no evidence of significant temperature dependence of OSLDs used as passive dosimeters over temperature ranges that could reasonably be expected to occur in a practical situation.

Edmund and Andersen (2007) investigated in more detail the effect of irradiation and readout temperature of Al_2O_3:C crystals used as probes in an optical fiber system. The authors concluded that there is a temperature dependence due to the effect of shallow traps and thermal excitation, but the dependence is crystal dependent and relatively small (−0.2–0.6% per degree Celsius, depending on the sample). In dosimetry using optical fibers the authors recommend that calibration and measurement of the OSL probes are carried out at the same temperature of irradiation.

3.1.8. Directional, dose rate and field-size dependence. InLight Dot dosimeters showed no directional dependence within the experimental uncertainties (0.9%) for dosimeters irradiated inside a water-equivalent cylindrical phantom from different directions (Jursinic 2007). There also seems to be no dependence on the dose rate for clinical linear accelerators (Jursinic 2007, Yukihara *et al* 2007, Viamonte *et al* 2008). In terms of the field-size dependence, the results are identical to ionization chamber measurements within experimental uncertainties (Yukihara *et al* 2007, Viamonte *et al* 2008).

3.2. Radiodiagnostics

The use of OSLDs as passive dosimeters in quality control and *in vivo* dosimetry in radiodiagnostics is relatively similar to TLDs. This may explain the small number of reports on

this topic in the literature when compared to applications in radiotherapy. The main problem in x-ray dosimetry using Al_2O_3:C is its over-response to low-energy x-rays with respect to tissue, caused by its effective atomic number (see section 2.6). However, appropriate calibration in a similar radiation field is sufficient to solve this problem as long as the energy spectrum is consistent with the field to be evaluated.

Some studies have been carried out on the performance of OSLDs in computed tomography (CT). Peakheart (2006) performed a series of tests of Luxel^{TM} passive dosimeters and a real-time optical fiber system based on KBr:Eu optical fiber probes (Gaza and McKeever 2006). Some of the properties investigated were the linearity with tube current at various tube voltages in air, at the center of a CT body phantom and at different organ sites inside an anthropomorphic phantom. The Luxel^{TM} response was linear with tube current and the standard deviation of the measurements was typically better than 6%. The beam profile at the center of the CT body phantom was successfully measured using OSLDs irradiated at different positions along the axis of the phantom. Using the KBr:Eu optical fiber system, the results were obtained in real time with a precision typically better than 3% and the beam profile was measured using multiple irradiations. However, both Al_2O_3:C and KBr:Eu exhibit an energy dependence, varying between 20 and 30% in the range of kVp from 80 kV and 140 kV.

Recently Landuer Inc. started offering a service to measure the dose profile in CT scanners using a 15 cm long OSL strip. The OSL strip is placed in a plastic cylinder (12 mm diameter by 175 mm length) which can be inserted in the CT body phantom. After exposure, the OSL strip is read using a custom-made reader which scans the strip with a laser to obtain the dose profile with a resolution of 0.1 mm and the computed tomography dose index $CTDI_{100}$ is then calculated. Beam profiles obtained for helical scans using these OSL strips were used by Dixon and Ballard (2007) as supporting data for visualization of the measurement field in the peripheral axis of a CT body phantom and comparison of the periodicity in the dose distribution with the typical size of the ionization chamber used in the measurements.

Aznar *et al* (2005a) described tests of an optical fiber system that uses Al_2O_3:C OSL probes to determine the entrance and exit doses in mammography. The system is identical to that shown in figure 6 and uses the 'RL and post-irradiation OSL' readout protocol. The reproducibility was of the order of 3% at an air kerma of 4.5 mGy and the response was linear over the range investigated (4.5–30 mGy). However, because of the photon energy dependence of Al_2O_3:C the response increased 18% with an increase in the tube potential from 23 kV to 35 kV. This energy dependence was modeled using Monte Carlo calculations (Aznar *et al* 2005b). The authors also state that three radiologists separately evaluated the radiography images and considered that the probes did not compromise the evaluation of the mammogram images because of their distinct shape and small size.

3.3. Heavy charged particle dosimetry

The Al_2O_3:C OSL efficiency is well characterized for particles with energy of the order of hundreds of MeV per nucleon and LET values higher than $\sim$2 keV μm^{-1}, but it has not yet been sufficiently and precisely characterized for proton or carbon therapy applications yet. Only a few data points are currently available for Al_2O_3:C Luxel^{TM} used as passive dosimeters (figure 17). Sawakuchi *et al* (2008) compared the Al_2O_3:C OSL dose response to high-energy protons (1 GeV/u) and beta rays and concluded that the response is similar in each case. The authors also showed that the supralinearity observed in the total OSL signal when the measurements are carried out using Hoya U-340 filters can be eliminated by introducing an extra UV blocking filter (Schott WG-360), which removes the Al_2O_3:C UV emission band.

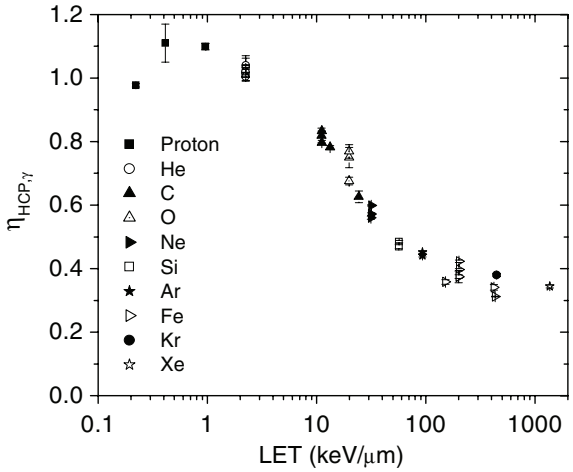

Figure 17. Luminescence response (efficiency) values $\eta_{HCP,\gamma}$ for Al_2O_3:C Luxel^{TM} dosimeters irradiated with HCP relative to gamma radiation. The data were obtained using the total OSL signal. The measurements were performed using a Risø TL/OSL-DA-15 reader with green stimulation and Hoya U-340 filters in front of the PMT (Yukihara *et al* 2006).

This result highlights the importance of choosing an appropriate optical filter for the OSL measurements.

The Al_2O_3:C properties for proton dosimetry were also investigated by Andersen *et al* (2007) and Edmund *et al* (2007). In certain conditions (doses less than 0.3 Gy and Al_2O_3:C crystals of dimensions 2 mm × 0.5 mm × 0.5 mm), the initial OSL intensity seemed to be independent of the proton energy. The luminescence efficiency was observed to depend on the particular crystal used in the probe and on the choice of integration period of the OSL curve.

At this point, research on the use of OSL in proton and carbon therapy dosimetry is at an early stage. More systematic studies are required if the technique is to be fully developed for this application.

4. Conclusions and final remarks

As with any technique, advances in OSL dosimetry in different fields require an understanding of the interplay between material properties, experimental protocols, theoretical aspects and practical aspects. This paper reviewed some of the theoretical and practical aspects in OSL dosimetry as applied to medicine. The current activity in the field is represented by an increasing number of publications and groups involved in this research. Most of the literature has been devoted to applications in radiotherapy, because of the need to investigate new and more convenient dosimeters to meet the challenging demands of increasingly complex radiation delivery approaches. However, investigations on the OSL technique applied to computed tomography, radiodiagnostics, and particle dosimetry are starting to appear and will likely increase in the future.

Several reports highlight the characteristics of OSLD as being suitable for radiotherapy applications. OSLDs are small and capable of providing dose estimates with an uncertainty of the order of 0.7–3.2%, depending on the readout equipment and methodology. Other important aspects are the possibility of re-estimating the absorbed doses, and the small or no

dependence on beam quality, temperature and angle of irradiation. Furthermore, there is the possibility of using OSL materials as probes for remote, *in vivo* dosimetry. The dose response becomes supralinear for doses above ∼2 Gy, but in general this can be compensated by using an appropriate calibration curve or by the use of a methodology that takes into account the sensitivity changes in the material. The sensitivity change as a function of irradiation history is one of the most important effects to consider, principally when adopting individual dosimeter calibration. Methodologies to cope with these sensitivity changes exist, but they have only been demonstrated in limited operational modalities. There are still aspects to be investigated, such as the stability of the OSL signal and the possibility of re-using the dosimeters.

Important progress has been achieved in optical fiber dosimetry using OSL probes, allowing precise *in vivo* dose estimations. Some of the problems that have been addressed are the sensitivity changes and temperature dependence of the OSL signal. Although such systems have been used experimentally in a clinical setting, a commercial system is still not available.

The development of new materials may also contribute to advances in OSL dosimetry by providing material with properties suitable for each type of application, such as better tissue equivalency for radiodiagnostics or faster bleaching times for optical fiber dosimetry. However, OSL materials often fade over different time scales due to the presence of shallow traps. This is due to one of the disadvantages of the OSL technique: the fact that the optical stimulation simultaneously releases charges from different trapping centers, including shallow traps.

The availability and capability of OSL readers has improved over time with the introduction of new dosimetry systems and portable readers. However, except for automated research readers, all new instruments are based on Al_2O_3:C. New materials and readers, including optical fiber systems, will likely increase the acceptance and availability of OSL systems in a wider variety of environments and clinical settings.

Few investigations are available on the application of OSL to proton or carbon therapy dosimetry. This is an area where new dosimetry techniques with high precision and spatial resolution to validate treatment planning calculations are in demand, since most detectors (at the moment, even TLDs and OSLDs) suffer from changes in response or efficiency with the energy of the beam.

In conclusion, current advances and characterization of OSLDs are providing increasing confidence on the application of the OSL technique to fields other than personal dosimetry. The most outstanding problem is the lack of widespread agreement on best practices. Nevertheless, OSL represents an additional tool available for medical physicists and researchers, offering advantages and convenience in a number of situations. The fact that in specific situations OSLDs do not seem to require corrections for angle of irradiation, energy and temperature greatly simplifies their clinical use, potentially representing a key benefit of the OSL technology.

Acknowledgments

The authors would like to thank Claus Andersen (Risø National Laboratory), Joanna Izewska (International Atomic Energy Agency), Cliff Yanhke (Landauer Inc.), Gabriel Sawakuchi and David Peakheart for the comments on the manuscript. We also would like to express our gratitude to our collaborators at the University of Oklahoma Health Sciences Center, in particular Salahuddin Ahmad and Chun Ruan, for their support and encouragement.

References

Akselrod A E and Akselrod M S 2002 Correlation between OSL and the distribution of TL traps in Al_2O_3:C *Radiat. Prot. Dosim.* **100** 217–20

Akselrod M S, Bøtter-Jensen L and McKeever S W S 2007 Optically stimulated luminescence and its use in medical dosimetry *Radiat. Meas.* **41** S78–99

Akselrod M S and Gorelova E A 1993 Deep traps in highly sensitive a-Al_2O_3:C TLD crystals *Nucl. Tracks Radiat. Meas.* **21** 143–6

Akselrod M S, Kortov V S, Kravetsky D J and Gotlib V I 1990 Highly sensitive thermoluminescent anion-defect α-Al_2O_3:C single crystal detectors *Radiat. Prot. Dosim.* **33** 119–22

Akselrod M S and McKeever S W S 1999 A radiation dosimetry method using pulsed optically stimulated luminescence *Radiat. Prot. Dosim.* **81** 167–76

Andersen C E, Aznar M C, Bøtter-Jensen L, Bäck S Å J, Mattsson S and Medin J 2003 Development of optical fibre luminescence techniques for real time *in vivo* dosimetry in radiotherapy *Int. Symp. on Standards and Codes of Practice in Medical Radiation Dosimetry (Vienna: IAEA)* pp 353–60

Andersen C E, Edmund J M, Medin J, Grusell E, Jain M and Mattsson S 2007 Medical proton dosimetry using radioluminescence from aluminium oxide crystals attached to optical fiber cables *Nucl. Instrum. Methods Phys. Res.* A **580** 466–8

Andersen C E, Marckmann C J, Aznar M C, Bøtter-Jensen L, Kjær-Kristoffersen F and Medin J 2006 An algorithm for real-time dosimetry in intensity-modulated radiation therapy using the radioluminescence signal from Al_2O_3:C *Radiat. Prot. Dosim.* **120** 7–13

Aznar M C, Andersen C E, Bøtter-Jensen L, Bäck S Å J, Mattsson S, Kjær-Kristoffersen F and Medin J 2004 Real-time optical-fibre luminescence dosimetry for radiotherapy: physical characteristics and applications in photon beams *Phys. Med. Biol.* **49** 1655–69

Aznar M C, Hemdal B, Medin J, Marckmann C J, Andersen C E, Bøtter-Jensen L, Andersson I and Mattsson S 2005a *In vivo* absorbed dose measurements in mammography using a new real-time luminescence technique *Br. J. Radiol.* **78** 328–34

Aznar M C, Medin J, Hemdal B, Thilander Klang A, Bøtter-Jensen L and Mattsson S 2005b A Monte Carlo study of the energy dependence of Al_2O_3:C crystals for real-time *in vivo* dosimetry in mammography *Radiat. Prot. Dosim.* **114** 444–9

Bloom D, Evans D R, Holmstrom S A, Polf J C, McKeever S W S and Whitley V 2003 Characterisation of Al_2O_3 single crystals grown by the laser-heated pedestal growth technique for potential use in radiation dosimetry *Radiat. Meas.* **37** 141–9

Bos A J J 2001 High sensitivity thermoluminescence dosimetry *Nucl. Instrum. Methods Phys. Res.* B **184** 3–28

Bos A J J, Prokić M and Brouwer J C 2006 Optically and thermally stimulated luminescence characteristics of MgO:Tb^{3+} *Radiat. Prot. Dosim.* **119** 130–3

Bøtter-Jensen L 1997 Luminescence techniques: instrumentation and methods *Radiat. Meas.* **27** 749–68

Bøtter-Jensen L, Agersnap Larsen N, Markey B G and McKeever S W S 1997 Al_2O_3:C as a sensitive OSL dosemeter for rapid assessment of environmental photon dose rates *Radiat. Meas.* **27** 295–8

Bøtter-Jensen L, McKeever S W S and Wintle A G 2003 *Optically Stimulated Luminescence Dosimetry* (Amsterdam: Elsevier)

Bube R H 1960 *Photoconductivity of solids* (New York: Wiley))

Bulur E 1996 An alternative technique for optically stimulated luminescence (OSL) experiment *Radiat. Meas.* **26** 701–9

Bulur E and Göksu H Y 1998 OSL from BeO ceramics: new observations from an old material *Radiat. Meas.* **29** 639–50

Damkjær S M S, Andersen C E and Aznar M C 2007 Improved real-time dosimetry using the radioluminescence signal from Al_2O_3:C *Radiat. Meas.* **43** 893–7

Dixon R L and Ballard A C 2007 Experimental validation of a versatile system of CT dosimetry using a conventional ion chamber: beyond $CTDI_{100}$ *Med. Phys.* **34** 3399–413

Edmund J M and Andersen C E 2007 Temperature dependence of the Al_2O_3:C response in medical luminescence dosimetry *Radiat. Meas.* **42** 177–89

Edmund J M, Andersen C E, Greilich S, Sawakuchi G O, Yukihara E G, Jain M, Hajdas W and Mattsson S 2007 Optically stimulated luminescence from Al_2O_3:C irradiated with 10–60 MeV protons *Nucl. Instrum. Methods Phys. Res.* A **580** 210–3

Edmund J M, Andersen C E, Marckmann C J, Aznar M C, Akselrod M S and Bøtter-Jensen L 2006 CW-OSL measurement protocols using optical fibre Al_2O_3:C dosemeters *Radiat. Prot. Dosim.* **119** 368–74

Evans B D, Pogatshnik G J and Chen Y 1994 Optical properties of lattice defects in a-Al_2O_3 *Nucl. Instrum. Methods Phys. Res.* B **91** 258–62

Gaza R and McKeever S W S 2006 A real-time, high-resolution optical fibre dosemeter based on optically stimulated luminescence (OSL) of KBr:Eu, for potential use during the radiotherapy of cancer *Radiat. Prot. Dosim.* **120** 14–9

Gaza R, McKeever S W S and Akselrod M S 2005 Near-real-time radiotherapy dosimetry using optically stimulated luminescence of Al_2O_3:C: mathematical models and preliminary results *Med. Phys.* **32** 1094–102

Gaza R, McKeever S W S, Akselrod M S, Akselrod A, Underwood T, Yoder C, Andersen C E, Aznar M C, Marckmann C J and Bøtter-Jensen L 2004 A fiber-dosimetry method based on OSL from Al_2O_3:C for radiotherapy applications *Radiat. Meas.* **38** 809–12

Huntley D J, Godfrey-Smith D I and Thewalt M L W 1985 Optical dating of sediments *Nature* **313** 105–7

Huston A L, Justus B L, Falkenstein P L, Miller R W, Ning H and Altemus R 2001 Remote optical fiber dosimetry *Nucl. Instrum. Methods Phys. Res.* B **184** 55–67

Huston A L, Justus B L, Falkenstein P L, Miller R W, Ning H and Altemus R 2002 Optically stimulated luminescence glass optical fibre dosemeters *Radiat. Prot. Dosim.* **101** 23–6

Jursinic P A 2007 Characterization of optically stimulated luminescence dosimeters, OSLDs, for clinical dosimetric measurements *Med. Phys.* **34** 4594–604

Klein D M and McKeever S W S 2008 Optically stimulated luminescence from KBr:Eu as a near real-time dosimetry system *Radiat. Meas.* **43** 883–7

Lee K H and Crawford J H Jr 1979 Luminescence of the F center in sapphire *Phys. Rev.* B **19** 3217–21

Marckmann C J, Aznar M C, Andersen C E and Bøtter-Jensen L 2006 Influence of the stem effect on radioluminescence signals from optical fibre Al_2O_3:C dosemeters *Radiat. Prot. Dosim.* **119** 363–7

Markey B G, Colyott L E and McKeever S W S 1995 Time-resolved optically stimulated luminescence from a-Al_2O_3:C *Radiat. Meas.* **24** 457–63

McKeever S W S 2001 Optically stimulated luminescence dosimetry *Nucl. Instrum. Methods Phys. Res.* B **184** 29–54

McKeever S W S, Akselrod M S, Colyott L E, Agersnap Larsen N, Polf J C and Whitley V H 1999 Characterisation of Al_2O_3 for use in thermally and optically stimulated luminescence dosimetry *Radiat. Prot. Dosim.* **84** 163–8

McKeever S W S, Akselrod M S and Markey B G 1996 Pulsed optically stimulated luminescence dosimetry using α-Al_2O_3:C *Radiat. Prot. Dosim.* **65** 267–72

McKeever S W S, Bøtter-Jensen L, Agersnap Larsen N and Duller G A T 1997 Temperature dependence of OSL decay curves: experimental and theoretical aspects *Radiat. Meas.* **27** 161–70

McKeever S W S and Moscovitch M 2003 On the advantages and disadvantages of optically stimulated luminescence dosimetry and thermoluminescence dosimetry *Radiat. Prot. Dosim.* **104** 263–70

McKeever S W S, Moscovitch M and Townsend P D 1995 *Thermoluminescence Dosimetry Materials: Properties and Uses* (Ashford: Nuclear Technology Publishing)

Miller S D and Murphy M K 2007 Technical performance of the Luxel Al_2O_3:C optically stimulated luminescence dosemeter element at radiation oncology and nuclear accident dose levels *Radiat. Prot. Dosim.* **123** 435–42

Mobit P, Agyingi E and Sandison G 2006 Comparison of the energy-response factor of LiF and Al_2O_3 in radiotherapy beams *Radiat. Prot. Dosim.* **119** 497–9

Molnar G, Benabdesselam M, Borossay J, Iacconi P, Lapraz D and Akselrod M S 2002 Influence of the irradiation temperature on the dosimetric and high temperature TL peaks of Al_2O_3:C *Radiat. Prot. Dosim.* **100** 139–42

Pagonis V, Chen R and Lawless J L 2006 Nonmonotonic dose dependence of OSL intensity due to competition during irradiation and readout *Radiat. Meas.* **41** 903–9

Peakheart D W 2006 Evaluation of clinically feasible dosimetry systems for CT quality assurance and dose optimization *MS Thesis* University of Oklahoma Health Sciences Center

Perks C A, Le Roy G and Prugnaud B 2007 Introduction of the InLight monitoring service *Radiat. Prot. Dosim.* **125** 220–3

Polf J C, McKeever S W S, Akselrod M S and Holmstrom S 2002 A real-time, fibre optic dosimetry system using Al_2O_3 fibres *Radiat. Prot. Dosim.* **100** 301–4

Polf J C, Yukihara E G, Akselrod M S and McKeever S W S 2004 Real-time luminescence from Al_2O_3 fiber dosimeters *Radiat. Meas.* **38** 227–40

Ranchoux G, Magne S, Bouvet J P and Ferdinand P 2002 Fibre remove optoelectronic gamma dosimetry based on optically stimulated luminescence of Al_2O_3:C *Radiat. Prot. Dosim.* **100** 255–60

Rowlands J A 2002 The physics of computed radiography *Phys. Med. Biol.* **47** R123–66

Sanderson D C W and Clark R J 1994 Pulsed photostimulated luminescence of alkali feldspars *Radiat. Meas.* **23** 633–9

Sawakuchi G O, Yukihara E G, McKeever S W S and Benton E R 2008 Optically stimulated luminescence fluence response of Al_2O_3:C dosimeters exposed to different types of radiation *Radiat. Meas.* **43** 194–8

Schembri V and Heijmen B J M 2007 Optically stimulated luminescence (OSL) of carbon-doped aluminum oxide (Al_2O_3:C) for film dosimetry in radiotherapy *Med. Phys.* **34** 2113–8

Sommer M, Freudenberg R and Henniger J 2007 New aspects of a BeO-based optically stimulated luminescence dosimeter *Radiat. Meas.* **42** 617–20

Sommer M and Henniger J 2006 Investigation of a BeO-based optically stimulated luminescence dosimeter *Radiat. Prot. Dosim.* **119** 394–7

Viamonte A, da Rosa L A R, Buckley L A, Cherpak A and Cygler J E 2008 Radiotherapy dosimetry using a commercial OSL system *Med. Phys.* **35** 1261–6

Whitley V H and McKeever S W S 2001 Linearly modulated photoconductivity and linearly modulated optically stimulated luminescence measurements on Al_2O_3:C *J. Appl. Phys.* **90** 6073–83

Yoshimura E M and Yukihara E G 2006 Optically stimulated luminescence: searching for new dosimetric materials *Nucl. Instrum. Methods Phys. Res.* B **250** 337–41

Yukihara E G, Mardirossian G, Mirzasadeghi M, Guduru S and Ahmad S 2007 Evaluation of Al_2O_3:C optically stimulated luminescence (OSL) dosimeters for passive dosimetry of high-energy photon and electron beams in radiotherapy *Med. Phys.* **35** 260–9

Yukihara E G and McKeever S W S 2006a Ionization density dependence of the optically and thermally stimulated luminescence from Al_2O_3:C (INVITED) *Radiat. Prot. Dosim.* **119** 206–17

Yukihara E G and McKeever S W S 2006b Spectroscopy and optically stimulated luminescence of Al_2O_3:C using time-resolved measurements *J. Appl. Phys.* **100** 083512

Yukihara E G, Sawakuchi G O, Guduru S, McKeever S W S, Gaza R, Benton E R, Yasuda N, Uchihori Y and Kitamura H 2006 Application of optically stimulated luminescence (OSL) technique in space dosimetry *Radiat. Meas.* **41** 1126–35

Yukihara E G, Whitley V H, McKeever S W S, Akselrod A E and Akselrod M S 2004 Effect of high-dose irradiation on the optically stimulated luminescence of Al_2O_3:C *Radiat. Meas.* **38** 317–30

Yukihara E G, Whitley V H, Polf J C, Klein D M, McKeever S W S, Akselrod A E and Akselrod M S 2003 The effects of deep trap population on the thermoluminescence of Al_2O_3:C *Radiat. Meas.* **37** 627–368

Yukihara E G, Yoshimura E M, Lindstrom T D, Ahmad S, Taylor K K and Mardirossian G 2005 High-precision dosimetry for radiotherapy using the optically stimulated luminescence technique and thin Al_2O_3:C dosimeters *Phys. Med. Biol.* **50** 5619–28